Sec6 mutations and the *Drosophila* exocyst complex

Mala Murthy[1,*], Ravi Ranjan[1,‡], Natalie Denef[2], Misao E. L. Higashi[1], Trudi Schupbach[2] and Thomas L. Schwarz[1,§]

[1]Division of Neuroscience, Children's Hospital, Harvard Medical School, Boston, MA 02115, USA
[2]Howard Hughes Medical Institute, Molecular Biology Department, Princeton University, Princeton, NJ 08544, USA
*Present address: Division of Biology, MC 139-74, Caltech, Pasadena, CA 91125, USA
‡Present address: Department of Pharmacology, University of Texas Health Sciences Center, San Antonio, TX 78229, USA
§Author for correspondence (thomas.schwarz@childrens.harvard.edu)

Accepted 11 November 2004
Journal of Cell Science 118, 1139-1150 Published by The Company of Biologists 2005
doi:10.1242/jcs.01644

Summary

To allow a detailed analysis of exocyst function in multicellular organisms, we have generated *sec6* mutants in *Drosophila*. We have used these mutations to compare the phenotypes of *sec6* and *sec5* in the ovary and nervous system, and we find them to be similar. We also find that Sec5 is mislocalized in *sec6* mutants. Additionally, we have generated an epitope-tagged Sec8 that localized with Sec5 on oocyte membranes and was mislocalized in *sec5* and *sec6* germ-line clones. This construct further revealed a genetic interaction of *sec8* and *sec5*. These data, taken together, provide new information about the organization of the exocyst complex and suggest that Sec5, Sec6 and Sec8 act as a complex, each member dependent on the others for proper localization and function.

Key words: Sec6, Sec5, Sec8, Oogenesis, Membrane trafficking

Introduction

Studies of the exocyst complex in yeast have benefited from an abundance of mutations in each member of the complex. The eight subunits of the exocyst (Sec3, Sec5, Sec6, Sec8, Sec10, Sec15, Exo70 and Exo84) were first identified in a screen that isolated conditional mutations in genes required for exocytosis. Mutations of each have been shown to prevent exocytosis and to arrest growth of the daughter cell and cytokinesis (Finger and Novick, 1998; Novick et al., 1980). The similarities of the phenotypes and extensive biochemical characterization have led to a model in which the complex functions as an integral unit that can interact with both plasma membranes and transport vesicles, and that, as a unit, marks sites of membrane insertion (Finger et al., 1998; Finger and Novick, 1997; Haarer et al., 1996; Mondesert et al., 1997).

In higher organisms, the investigation of the exocyst has been hampered by a lack of mutations. A mutation in murine *sec8* causes lethality shortly after gastrulation of the embryo, precluding a detailed analysis of the role of the complex (Friedrich et al., 1997). Recently, we have characterized *Drosophila sec5* mutations. As in yeast, Sec5 localization in *Drosophila* undergoes dynamic changes correlating with the sites at which it is required for the traffic of membrane proteins during oogenesis and cellularization. In homozygous *sec5* larvae and germ-line clones of *sec5* alleles, we observed defects in trafficking proteins to the plasma membrane (Murthy et al., 2003; Murthy and Schwarz, 2004).

In contrast to these genetic studies, investigation of other components of the exocyst has depended on the introduction of antibodies and the overexpression of wild-type or mutated forms of the proteins in wild-type genetic backgrounds. From these studies, some discrepancies in the localization of exocyst proteins and their phenotypes have emerged. *Drosophila* Sec5 concentrates specifically at sites of membrane addition in both ovaries and embryos but, in normal rat kidney (NRK) cells, different monoclonal antibodies to Sec6 and Sec8 recognized the exocyst complex at either the trans-Golgi network (TGN) or the plasma membrane (Yeaman et al., 2001). Furthermore, Exo70 associates with microtubules at the microtubule-organizing center in undifferentiated PC12 cells (Vega and Hsu, 2001), and Sec10 has been found both at the endoplasmic reticulum (ER) (Lipschutz et al., 2003) and on tubulo-vesicular extensions of the TGN and recycling endosomes (Prigent et al., 2003). Finally, an interaction between Sec8, SAP102 and the N-methyl-D-aspartate receptor (NMDAR) in mammalian neurons was found in the ER (Sans et al., 2003).

Indeed, although biochemical studies in yeast and neurons suggest the presence of only one copy of each subunit per complex (Hsu et al., 1996; TerBush et al., 1996) and the isolation of the exocyst complex from all yeast exocyst mutants shows that its structure is altered (TerBush and Novick, 1995), there is growing evidence that the members of the exocyst might not always act as a complex. For example, whereas *Drosophila sec5* mutations blocked the transport of many proteins to the plasma membrane of neurons and developing oocytes, the addition of antibodies specific for TGN-bound exocyst complexes to semi-intact NRK cells resulted in cargo accumulation in a perinuclear region (Yeaman et al., 2001). Also, the introduction of a dominant negative Sec10 or Sec5 small interfering RNA to NRK cells causes morphological changes and phenotypes at the recycling endosome (Prigent et al., 2003). Finally, the overexpression of Sec10 affects protein synthesis in MDCK cells by an interaction with an ER translocon (Lipschutz et al., 2000; Lipschutz et al., 2003) and yeast Sec10p and Sec15p might form a subcomplex (Guo et al., 1999). These findings raise the possibility that different complex members have different functions within the cell and might not always function as a unit.

The present uncertainty about the significance of exocyst subunits in multicellular organisms might, in part, arise from a lack of loss-of-function mutations that can be directly compared. In the present study, we report the isolation of a *sec6* mutation in *Drosophila* whose phenotype is comparable to that of *sec5*. Moreover, with antibodies to Sec5 and an epitope-tagged *sec8* transgene, we determine the interdependency of these complex members for their subcellular localization.

Materials and Methods

Isolation of *sec6* alleles

From the P-element-carrying line *w/w; EP2021/EP2021*, virgin females were crossed to males of the transposase-expressing line *w; CyO/+; Δ2-3, Sb/+*. From the progeny of this cross, 400 male *w; EP2021/CyO*; *Δ2-3, Sb/+* progeny were selected and individually mated to *w; Sco/CyO* females. Then, 64 white-eyed, curly-winged male progeny (*Ex/CyO*) from independent lines were selected and crossed to *w; Sco/CyO* females to establish balanced stocks. For each line, *Ex/CyO* males and females were mated and 15 lines were identified in which *Ex/Ex* was lethal. Three of these (*Ex15*, *Ex212* and *Ex228*) were also lethal over *Df(2R)PC4*. The molecular characterization of the *Ex15*, *Ex228* and *Ex212* alleles (Fig. 1) was performed with the following primers: 1, 5′-ATGGAGAATCTGAAGCAC-3′ in *sec6*; 2, 5′-TAGGAGGTCAGGAAGGTGTT-3′ in *Eip55E*; 3, 5′-GAATGGATGACCAAGGCCGC-3′ in *sec6*; 4, 5′-CGCTGTATCCGTATGCCTGCTC-3′ in *Eip55E*; 5, 5′-CCCTAAGCTTTTGTATGTTCTTATGCCTTC-3′ in CG30332; 6, 5′-GAATCCGAAAAGGAAAAGGACAGGTC-3′ in CG30122.

Drosophila stocks and clones

The following genotypes were used.
w; FRT42D sec6^{Ex15}/Cyo, GFP[Kr-Gal4, UAS-GFP]
w; FRT42D sec6^{Ex212}/Cyo, GFP
w; FRT40 ovo^{D}/FRT40 sec5^{E10} or *sec5^{E13}; nanos-Gal4/UAS-FLP*
w; FRT42B ovo^{D}/FRT42D sec6^{Ex15}; nanos-Gal4/UAS-FLP
w, hs-FLP; FRT42D Ubi-GFP/FRT42D sec6^{Ex15}
y, w, hs-FLP; FRT40 ovoD/FRT40 sec5^{E13}; nanos-Gal4/UAS-HA-Sec8
w, hs-FLP; FRT42D Ubi-GFP/FRT42D sec6^{Ex15}; nanos-Gal4/UAS-HA-Sec8
y, w, hs-FLP; FRT40 sec5^{E13}/Cyo; nanos-Gal4/UAS-HA-Sec8
UAS-HA-sec8 (III)

To generate the plasmid p[UASp-HA-sec8], we amplified the open reading frame of *sec8* from expressed sequence tag clone GM30905 using the 5′ primer 5′-TTTTCTAGAATGGACGCCCCACCGCCCACG-3′ and the 3′ primer 5′-TTTGCGGCCGCCTACACAACTACTCCCTTCGAGGG-3′, and digested it with *Xba*I and *Not*I. The resultant fragment was cloned into pBS-HA, and then cut with *Kpn*I and *Not*I. The HA-*sec8* fragment [N-terminal fusion of a triple hemagglutinin (HA) tag and *sec8*] was cloned into p[UASp].

Germ-line clones were generated both by using the dominant female sterile technique, involving *ovo^{D}*, and by looking for green-fluorescent-protein-deficient (*GFP$^{–}$*) clones. We did this because *ovo^{D}* had been recombined onto a *FRT42B* chromosome, and our *sec6* mutations had been recombined onto *FRT42D*. Because a chromosomal deletion between 42B and 42D might cause a phenotype on its own, we also generated germ-line clones using *FRT42D Ubi-GFP*. In this way, *GFP$^{–}$* egg chambers were homozygous mutant only for *sec6*, with no other chromosomal deletion. The phenotypes using both methods were identical, indicating that heterozygosity for the 42B-42D deletion is of no consequence to egg chambers within the context of the assays below and others (T. S., unpublished). For generating germ-line clones by heat shock, vials were placed for ~30 minutes per day at 37°C during larval and pupal development.

The trafficking assay used the following stocks.
w; FRT40 sec5^{E10}/CyO, GFP; UAS-CD8-GFP
w; FRT40 sec5^{E10}/CyO, GFP; elav-Geneswitch
w; sec6^{Ex15}/Cyo, GFP; UAS-CD8-GFP
w; sec6^{Ex15}/Cyo, GFP; elav-Geneswitch
UAS-CD8-GFP (III)
elav-Geneswitch (III)

Larvae were isolated by collecting eggs on grape caps with yeast paste for 2 hours and then raised at room temperature. At 24 hours after egg laying (AEL), homozygous mutant larvae were chosen by an absence of the GFP marker and transferred to fresh yeast paste until 72 hours AEL. Control larvae were raised similarly and were *y,w* unless otherwise indicated.

Immunocytochemistry and microscopy

Ovaries from 1-4-day-old females were dissected in PBS and kept on ice. Ovaries were fixed in 6:1 heptane:FIX [FIX=4 volumes H_2O, 1 volume buffer B (100 mM potassium phosphate pH 6.8, 450 mM KCl, 150 mM NaCl, 20 mM $MgCl_2$), and 1 volume 37% formaldehyde] for 15 minutes. They were stained in PBS containing 0.5% bovine serum albumin, 0.1% Triton X-100 and 5% normal goat or donkey serum. Larvae were attached to Sylgard with Nexaband glue (Veterinary Products Laboratories) and dissected in PBS with pulled-glass dissecting needles, and subsequently fixed with 3.7% formaldehyde in buffer B. For the trafficking assay, Triton X-100 was omitted from washes and antibody incubations.

The following stains and primary antibodies were used: Texas Red-X phalloidin, Alexa Fluor 568 phalloidin, Hoechst 33342, Alexa-Fluor-488-conjugated mouse anti-HA (Molecular Probes), mouse anti-HA at 1:500 (BabCO), mouse anti-Gurken-1D12 (Developmental Studies Hybridoma Bank), mouse anti-Sec5 (ascites) 22A2 at 1:200 (Murthy et al., 2003), rat monoclonal anti-CD8α at 1:200 (CALTAG Laboratories), Cy5-conjugated goat anti-horseradish-peroxidase (anti-HRP) at 1:200 (Jackson Immunoresearch). Secondary antibodies used were: Cy3-conjugated goat anti-mouse and FITC-conjugated goat anti-mouse (Jackson Immunoresearch), Alexa Fluor 647 goat anti-mouse (Molecular Probes). For images of ovaries, confocal data were acquired as single images or as image stacks of multitracked separate channels with a Zeiss LSM 510 microscope.

The amount of Sec5 in the neuropil (Fig. 2) was estimated by drawing an approximately 900 μm^2 box within the neuropil of the ventral nerve cord, on one side of the commissures in single confocal sections and obtaining a value for mean pixel intensity.

Trafficking assays

We modified the methods for this trafficking assay from our earlier published version of the experiment performed on *sec5^{E10}* larvae (Murthy et al., 2003). Originally, we were not aware of leakage from the *elav-Geneswitch* driver and therefore did not take into account the mCD8-GFP that was expressed before introduction to the drug and before Sec5 maternal contribution ran down in the mutants. In this version, we aged larvae to the appropriate time points and then fed half of the larvae 0.5 mM RU486 (mifepristone, Sigma) dissolved in wet yeast paste and mixed with instant fly food and sucrose. The other half were fed regular yeast paste. We were then able to subtract uninduced values for GFP and surface mCD8 from induced values to obtain final values that reflected the expression and trafficking of mCD8-GFP after 72 hours AEL. In addition, originally for *sec5^{E10}* larvae, we had collected ten sections per image stack at variable step intervals. This method might have led to an overestimate of the amount of mCD8-GFP expression. In this version of the trafficking assay, we instead collected confocal sections at 2 μm intervals, with variable numbers of sections per image stack. The experiment was in all other ways identical to the published version. Finally, in our previous analysis, some values were inadvertently calculated as the

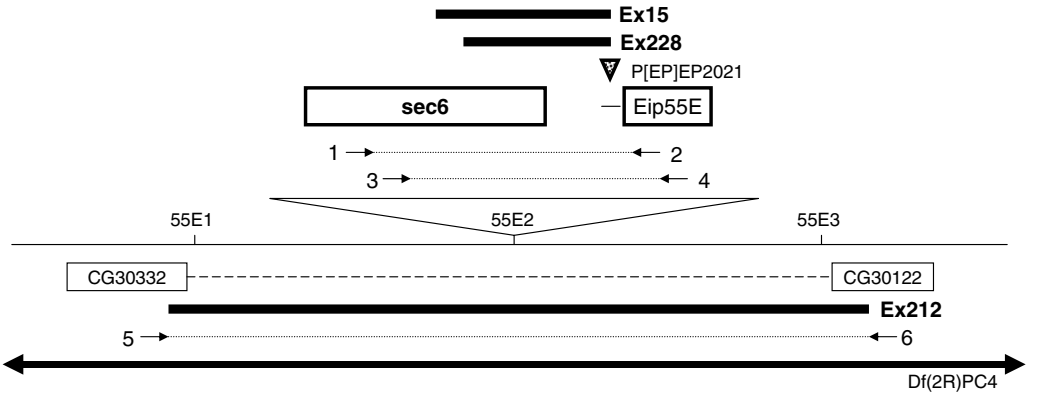

Fig. 1. Molecular characterization of *sec6* excisions. The genomic region 55E1-3 is shown, with an enlargement of the immediate vicinity of *sec6*. *Df(2R)PC4* was found to remove the *sec6* locus by in situ hybridization to polytene chromosomes (data not shown). The P-element EP2021 (small triangle), located just 3′ to *sec6* and within the 5′ untranslated region of the adjacent gene *Eip55E* was excised to give rise to three deletions, *Ex15*, *Ex228* and *Ex212* (heavy bars). Primers 1-6 were used to amplify DNA from these lines and the extent of the deleted regions was determined by DNA sequencing. Two of the three excisions, *Ex15* and *Ex228*, remove coding sequence from *sec6* and 21 base pairs of non-coding sequence from *Eip55E*. *Ex212* removes a 34 kb genomic fragment extending from predicted gene CG30332 to CG30122, as shown.

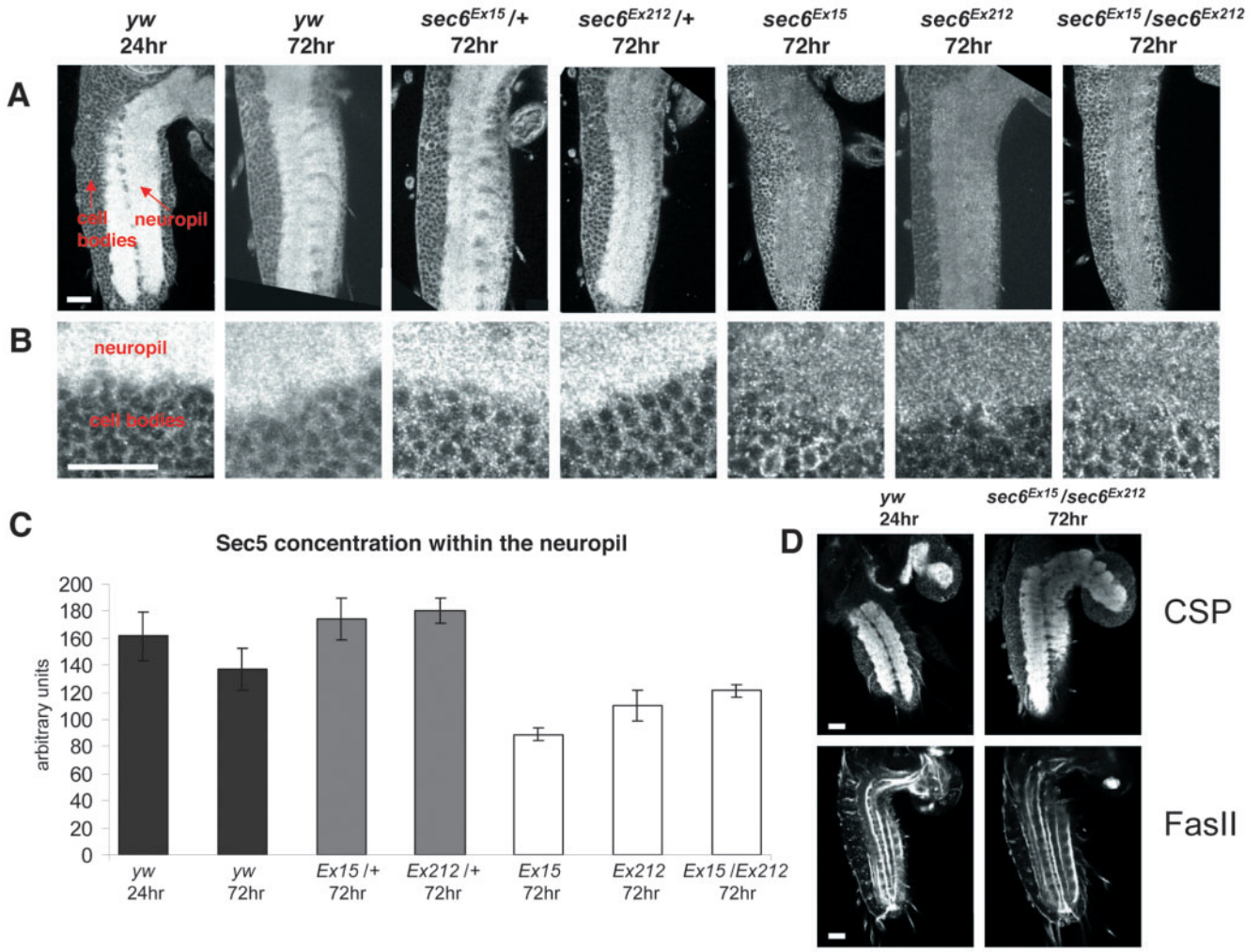

Fig. 2. Sec5 protein is mislocalized in *sec6* excision alleles. (A) Ventral nerve cords from *yw* larvae at 24 hours and 72 hours AEL, and $sec6^{Ex15}$/+, $sec6^{Ex212}$/+, $sec6^{Ex15}$, $sec6^{Ex212}$ and $sec6^{Ex15/Ex212}$ at 72 hours AEL. All nerve cords were stained for Sec5 with monoclonal antibody 22A2. All animals were imaged at the same image settings for comparison. (B) Close ups of the cell body and neuropil regions of the nerve cords from A. (C) Quantitation of mean pixel intensity for a fixed area of the neuropil region of nerve cords from *yw* 24 hours (n=6), *yw* 72 hours (n=4), $sec6^{Ex15}$/+ 72 hours (n=4), $sec6^{Ex212}$/+ 72 hours (n=5), $sec6^{Ex15}$ 72 hours (n=8), $sec6^{Ex212}$ 72 hours (n=5) and $sec6^{Ex15/Ex212}$ 72 hours (n=8). Statistical significance of the reduction of Sec5 in the mutant neuropil compared with the wild type is: P=0.008 ($sec6^{Ex15}$ 72 hours vs *yw* 24 hours); P=0.04 ($sec6^{Ex212}$ 72 hours vs *yw* 24 hours); P=0.07 ($sec6^{Ex15/Ex212}$ 72 hours vs *yw* 24 hours). (D) Ventral nerve cords from *yw* 24 hours AEL and $sec6^{Ex15}$/$sec6^{Ex212}$ 72 hours AEL were stained for cysteine string protein (CSP) and FasII. All scale bars are 20 μm.

maximum intensity pixel at each point within a projected *z*-axis stack. In the present analysis, we summed the pixels in the *z*-axis stack to obtain total pixel intensity for each channel.

Confocal data for these experiments were acquired as 2 μm interval image stacks of multitracked separate channels with a Zeiss LSM 510 microscope. Identical gain, offset, pinhole and laser settings were used for the mutant and control for each experiment. For quantification of total pixel intensity in cell bodies of bipolar dendrite (bd) sensory neurons, a region of interest (ROI) was drawn around the two cell bodies that lie next to one another for a given bd neuron in a peripheral segment, found in the Cy5 channel, and the sum of pixel intensities for that ROI across the *z*-axis stack calculated for each of three channels, Cy5 (HRP), Cy3 (CD8) and GFP. For background subtraction, an identical ROI was drawn outside the cell bodies.

Under these modified conditions, we also repeated the trafficking assay in the axons of bd neurons and at the boutons of the neuromuscular junction (NMJ). As before, we found reductions in surface mCD8 in $sec5^{E10}$ larvae. Surface mCD8 immunoreactivity was reduced in axons to 8% of control (9% when normalized to HRP; P=0.0001) and at the NMJ to 2% of control (1% normalized to HRP; P=0.0002). However, in both axons and the NMJ, the amount of mCD8-GFP expression was also reduced compared with the wild type. For sensory axons, an ROI was drawn along a portion of the axon and the sum of pixel intensities for each channel obtained after background subtraction. This sum was divided by the length in μm of the axon segment measured. For quantification of pixel intensity at synaptic boutons of the NMJ, an ROI was drawn around the entire endplate and total pixel intensity values for each channel calculated after background subtraction.

Statistics

All P values reported in this study are two-tailed values and derived from Student's t test, assuming unequal variances. For calculating standard error after subtracting two averages from each other, each with a standard error (as in Fig. 2F), we took the square root of the sum of the squares of the standard error from each average. To obtain the standard error after dividing two averages, i.e. for values normalized to either HRP- or GFP-intensity, we applied the following formula for the error on the ratio of two values, A and B:

$$\text{standard error of the mean on A/B} = 1/\text{B (standard error on A)} + \text{A/B}^2 \text{ (standard error on B)}.$$

We determined whether the normalized values were significantly different by finding values for test statistic (t) and degrees of freedom (df) according to the following formulae:

$$t = (q_1 - q_2) \div (v_1^2/n_1 + v_2^2/n_2)^{0.5}$$
$$df = (v_1^2/n_1 + v_2^2/n_2)^2 \div [(v_1^2/n_1)^2/n_1{-}1 + (v_2^2/n_2)^2/n_2{-}1],$$

where q_1 and q_2 are the normalized values for fluorescent intensity, v_1 and v_2 are the variances of those values, and n is the number of values in the data sets for the determination of the average intensities. From these values, we calculated a two-tailed P value by using the calculator at http://www.graphpad.com/quickcalcs/PValue1.cfm.

Results

Deletions of *sec6*

The *Drosophila* homolog of *sec6* is located at 55E (Murthy et al., 2003) and has a predicted open reading frame of 739 amino acids that are 21% identical to human *sec6* and 37% identical to yeast *sec6*. No other *sec6* gene is present in the sequenced *Drosophila* genome. This gene is removed by *Df(2R)PC4*. To obtain a specific mutation in *sec6*, we excised a P element, *EP2021*, located 1.2 kb downstream of the 3′ end of *sec6* and upstream of the adjacent predicted open reading frame, *Eip55E* (Fig. 1). We obtained three excision lines from this screen, *Ex15*, *Ex212* and *Ex228*. Amplification of genomic DNA isolated from homozygous *Ex15*, *Ex212* and *Ex228* larvae with the polymerase chain reaction primer pairs outlined in Fig. 1 allowed us to sequence across the deletions created by the imprecise excision of the P element. The *Ex15* deletion begins at amino acid 397 of Sec6 and continues to the 21st base pair in the 5′ untranslated region of the neighboring gene *Eip55E*. *Ex228* is a smaller deletion, extending from amino acid 541 of Sec6 to the 21st base pair of the 5′ untranslated region of *Eip55E*. *Ex212* carries a 38 kb deletion surrounding *sec6*. The deletion begins in the last exon of the gene *CG30332* and ends after the fifth intron of *CG30122*. This deletion removes eight genes, including *sec6*, between *CG30332* and *CG30122*. Because available anti-Sec6 antibodies do not work in *Drosophila*, we cannot determine directly whether a truncated form of Sec6 remains in the *sec6* excision alleles. However, the lethal periods and phenotypes of $sec6^{Ex15}$, $sec6^{Ex228}$ and $sec6^{Ex212}$ as homozygotes are identical to those of each allele over *Df(2R)PC4* or over one another; therefore, by genetic criteria, the three excision alleles are likely to be null. In addition to disrupting *sec6*, these excision are likely to interfere with expression of the *Eip55E* gene, an ecdysone-induced cystathionine γ-lyase expressed in fat bodies, salivary glands and lymph glands (Andres et al., 1993). The lethality of the excisions and the phenotypes discussed below are not attributable to *Eip55E*, because *Eip55E* mutants are viable and fertile.

Although flies homozygous for the original P element insert EP2021 are both viable and fertile, larvae either homozygous for $sec6^{Ex15}$ or trans-heterozygous for $sec6^{Ex15}$ and *Df(2R)PC4* or $sec6^{Ex15}$ and $sec6^{Ex212}$ die from growth arrest at 96 hours AEL, similar to the phenotype for $sec5^{E10}$, a null allele (Murthy et al., 2003). The *sec6* larvae, however, are much smaller than the *sec5* larvae. Whereas *sec5* larvae at the end of their lifespan are the size of wild-type larvae at 48 hours AEL, *sec6* larvae are never larger than wild-type larvae at 24 hours AEL. The $sec6^{Ex15}$ larvae, like the $sec5^{E10}$ larvae, probably survive to 96 hours AEL owing to the persistence of maternally contributed RNA and protein.

Sec5 is mislocalized in *sec6* mutants

Normally, Sec5 concentrates in the neuropil, the synapse-rich region of the nerve cord of first-instar larvae. We therefore used a previously characterized Sec5-specific antibody (Murthy et al., 2003) to determine whether Sec5 localization depends on the presence of Sec6. In 72-hour-AEL $sec6^{Ex15}/sec6^{Ex15}$, $sec6^{Ex212}/sec6^{Ex212}$ or $sec6^{Ex15}/sec6^{Ex212}$ larvae, Sec5 is present but greatly reduced in the neuropil when compared with either wild-type or heterozygous larvae (Fig. 2A,B). We quantified Sec5 in the neuropil and found it to be significantly reduced in the mutants compared with wild-type controls (Fig. 2C). This mislocalization is not due to a general disruption of the architecture of the central nervous system (CNS), which appeared to be grossly normal when $sec6^{Ex15}/sec6^{Ex212}$ larvae were stained for the synaptic vesicle marker cysteine string protein or for FasII, which labels axon tracts within the CNS. The mislocalization of Sec5 in the nerve cord of *sec6* mutants is therefore likely to be a specific effect on members of the exocyst complex.

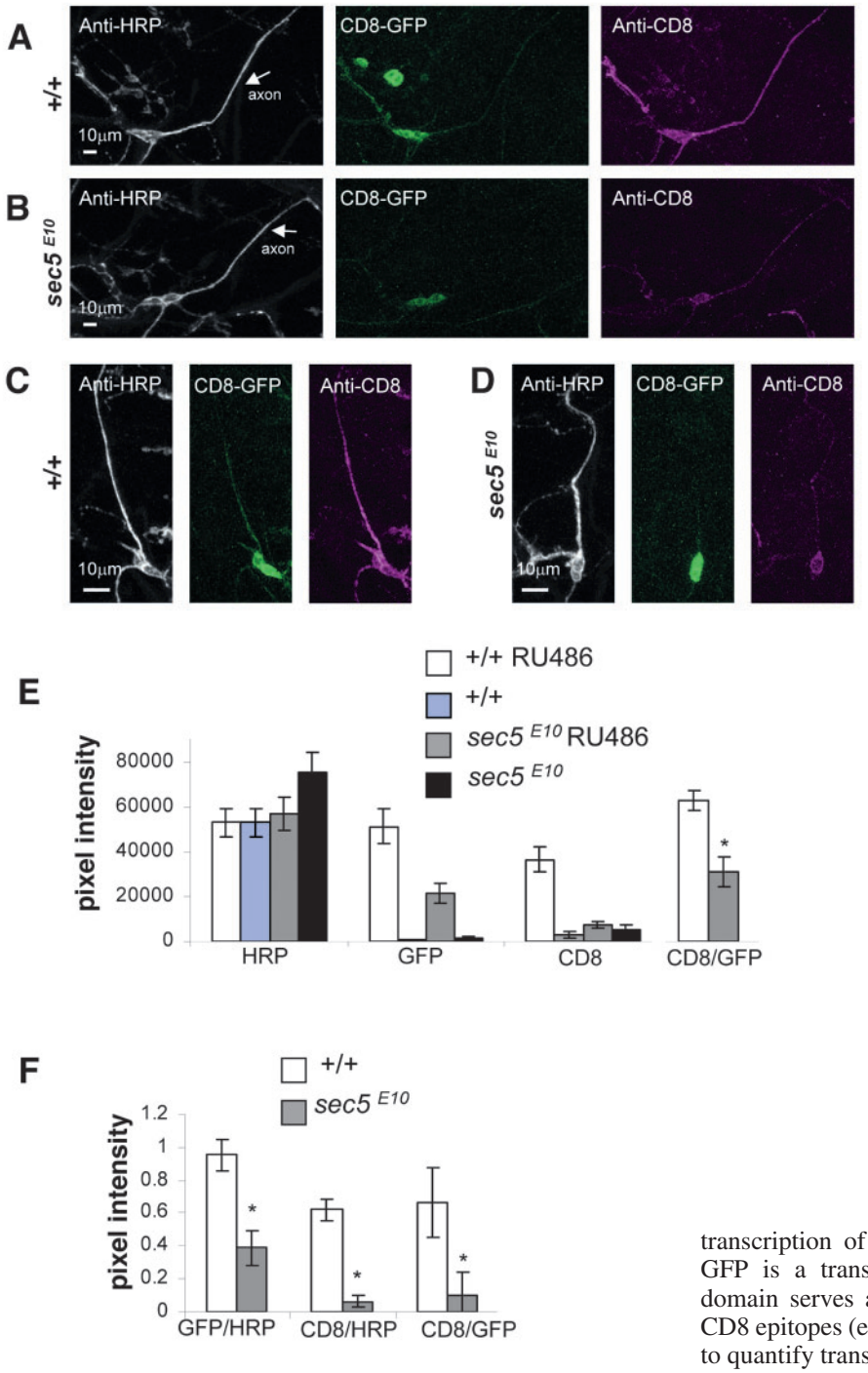

Fig. 3. Vesicle trafficking defects in *sec5*^{E10}. (A) A lateral bd sensory neuron in a wild-type larva that had been fed RU486 at 48 hours AEL and dissected at 59 hours AEL. Anti-HRP immunostaining (gray) was used to find bd sensory neurons in each animal. (B) A lateral bd neuron as in A but from a *sec5*^{E10} mutant fed RU486 at 72 hours AEL and dissected at 83 hours AEL. *sec5*^{E10} larvae show less cell surface CD8 than the control. (C,D) Additional wild-type and *sec5*^{E10} neurons as in A and B. (E) From quantitative fluorescent microscopy of the transport assay, surface-expressed CD8 immunofluorescence, total GFP fluorescence and cell surface area (measured by HRP immunoreactivity) were expressed as fluorescent units after background subtraction. In the sensory neuron soma [n=7 for wild-type larvae fed RU486 (white) and uninduced (blue); n=6 for *sec5*^{E10} larvae fed RU486 (gray) and uninduced (black)], there are comparable levels of anti-HRP labeling at the cell surface. Total GFP fluorescence is reduced in the RU486-fed mutants (gray) compared with RU486-fed controls (white), but there is a significant induction of the GFP signal, which is a measure of transgene expression, in the RU486-fed (gray) compared with uninduced (black) mutants. The amount of mCD8 at the cell surface is reduced in the RU486-fed mutants compared to RU486-fed controls, and a 50% reduction is observed when surface mCD8 is normalized to GFP in order to control for the level of transgene expression (P=0.004). (F) To measure the amount of transgene induction by feeding RU486, the uninduced averages (blue and black bars in E) were subtracted from the RU486-induced averages (white and gray bars in E). To control for differences in cell size, induced GFP and induced surface CD8 were then normalized to the anti-HRP signal. The amount of induced mCD8 trafficked to the cell surface was also normalized to the induced GFP signal, revealing the disruption of transport of the newly synthesized protein to the surface.

Defects in vesicle trafficking in *sec6* mutants

Because *sec5* mutations in *Drosophila*, like exocyst mutations in yeast, prevent membrane traffic to the cell surface, we hypothesized that a similar defect might occur in *sec6* mutants. To analyse *sec5* mutations, we developed an acute assay of membrane transport so as to examine the transport of newly synthesized proteins at the end of the mutants' lifespan, when maternally contributed Sec5 was no longer sufficient for cellular function (Murthy et al., 2003). The neuron-specific *elav* promoter was used to express the Geneswitch product, an inactive form of Gal4, in the nervous system. Upon feeding larvae RU486, Geneswitch is rendered active, which causes transcription of an mCD8-GFP-encoding transgene. mCD8-GFP is a transmembrane protein whose cytoplasmic GFP domain serves as a reporter of protein synthesis and whose CD8 epitopes (expressed on the surface of the cell) can be used to quantify transport to the surface; in the absence of Triton X-100, anti-mCD8 antibody binds only the subset of CD8 expressed on the cell surface, whereas the GFP fluorescence represents both surface and internal pools of the protein. We examined the lateral bd neurons in the peripheral nervous system because they were accessible to the antibody in the absence of Triton X-100. Animals were also stained with an anti-HRP antibody that labels a neuronal surface antigen so that the GFP and mCD8 signals could be normalized to the surface area of the cell.

Our previous use of this method (Murthy et al., 2003) might have overestimated the amount of transgene expression in the *sec5* mutant and also did not take into account the leakiness of the Geneswitch system, which permits a low level of transgene

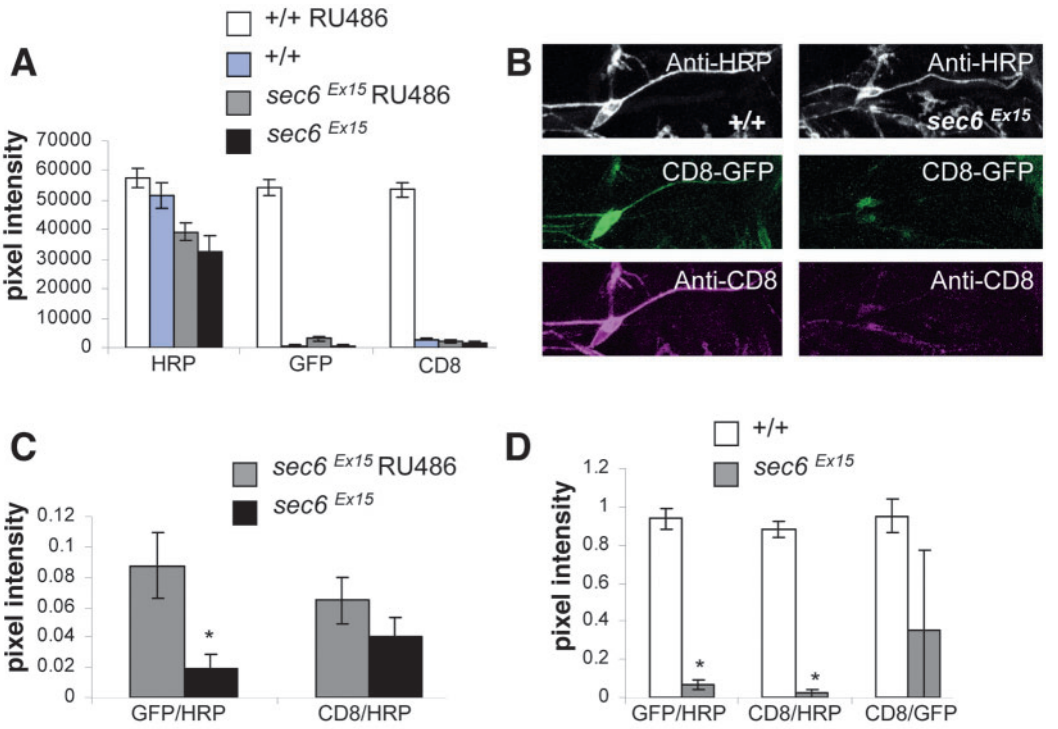

Fig. 4. Vesicle trafficking defects in *sec6*^{Ex15} larvae at 72 hours AEL. (A) From quantitative fluorescent microscopy of the transport assay in neuronal cell bodies, surface-expressed CD8 immunofluorescence, total GFP fluorescence and cell surface area (measured by HRP immunoreactivity) were expressed as fluorescent units after background subtraction. n=10 for wild-type larvae fed RU486 (white); n=8 for wild-type larvae uninduced (blue); n=13 for *sec6*^{Ex15} larvae fed RU486 (grey); and n=9 for uninduced *sec6*^{Ex15} larvae (black). (B) Representative lateral bd sensory neurons as used in the assay in A. In particular, a wild-type larva that had been fed RU486 at 24 hours AEL and dissected and stained in the absence of Triton X-100 at 36 hours AEL is compared with a *sec6*^{Ex15} mutant fed RU486 at 72 hours AEL similarly stained at 84 hours AEL. Anti-HRP immunostaining (gray) was used to find bd sensory neurons in each animal. The *sec6*^{Ex15} larvae show less cell surface CD8 than the control, but also showa large decrease in GFP fluorescence. (C) When normalized to the anti-HRP signal, there was a significant induction of the *mCD8-GFP* transgene in the *sec6*^{Ex15} mutant after feeding RU486 (P=0.01), but the amount of mCD8 at the soma surface was not significantly increased. (D) To measure the amount of transgene induction in the cell body by feeding RU486, the uninduced averages (blue and black bars in A) were subtracted from the RU486 averages (white and gray bars in A). To control for differences in cell size, GFP and surface CD8 were also normalized to the anti-HRP signal, as in C. The amount of induced mCD8 trafficked to the cell surface, when normalized to the corrected GFP signal, is decreased in the mutant compared with control.

expression even in the absence of RU486. Based on this information, we have made corrections to the methods and used the modified assay for a re-examination of *sec5*^{E10} and an examination of *sec6*^{Ex15}.

We repeated the trafficking analysis on *sec5*^{E10} larvae. These larvae were fed either plain or RU486-containing yeast paste from 72-83 hours AEL. Two types of controls were used for comparison: similarly sized larvae that had been fed either plain or RU486-containing food from 48-59 hours AEL (Fig. 3) or similarly aged larvae that had been fed from 72-83 hours AEL (data not shown). We observed a strong induction of the transgene in the somata of lateral bd neurons in both mutant and wild-type larvae (Fig. 3A-D). Although we noticed the presence of a moderate leak from the Geneswitch driver in *sec5*^{E10} and wild-type animals (such that, even when not fed RU486, both mutant and wild-type larvae showed some mCD8-GFP expression), there was a substantial induction of the transgene over this baseline in both mutant and control (Fig. 3E). When normalized to the HRP signal, the total induced GFP in the cell body and the total induced anti-mCD8 labeling at the surface of the cell body were reduced in the mutant to 41% (P=0.0019) and 10% (P<0.0001) of control, respectively (Fig. 3F). The amount of induced mCD8 at the cell surface, even when normalized to the amount of induced GFP in the soma, was still reduced in the mutant to 15% of control (P=0.0526; even if un-induced 'leak' is not subtracted, a 50% reduction is measured, P=0.004) (Fig. 3E). Thus, the reduction of mCD8 at the cell surface in the mutant was not due simply to a decrease in the amount of mCD8-GFP induction. Rather, confirming our earlier result, between 72 hours and 83 hours AEL in *sec5*^{E10} mutants, much less of the newly synthesized mCD8 is inserted at the membrane and a defect in the membrane-trafficking pathway is indicated.

The *sec6*^{Ex15} mutant larvae at 72 hours AEL were also fed either plain or RU486-containing yeast paste for 12 hours, and compared with similarly-sized control larvae fed at 24 hours AEL. Both control and mutant larvae, after introduction to the drug, showed expression of the transgene in the cell bodies of lateral bd neurons (Fig. 4A,B), but the amount of GFP fluorescence was greatly reduced in the mutant cells when compared to wild type.

The transport to the surface of the mCD8 reporter-gene product was measured as above (Fig. 4A-D). Although there was a 79% induction (P=0.01) of mCD8-GFP in *sec6* animals fed RU486 compared with animals that were not induced (Fig. 4C), there was no significant induction of mCD8 at the cell surface, indicating a defect in trafficking the protein to the cell surface at 72 hours AEL.

When we subtracted the levels of expression without RU486 from the RU486-induced levels for both the mutants and the wild type, and normalized these values to the HRP levels (Fig. 4D), the total induced GFP in the cell body and the total induced anti-mCD8 labeling at the surface of the cell body were reduced in the mutant to 7% (P<0.0001) and 3%

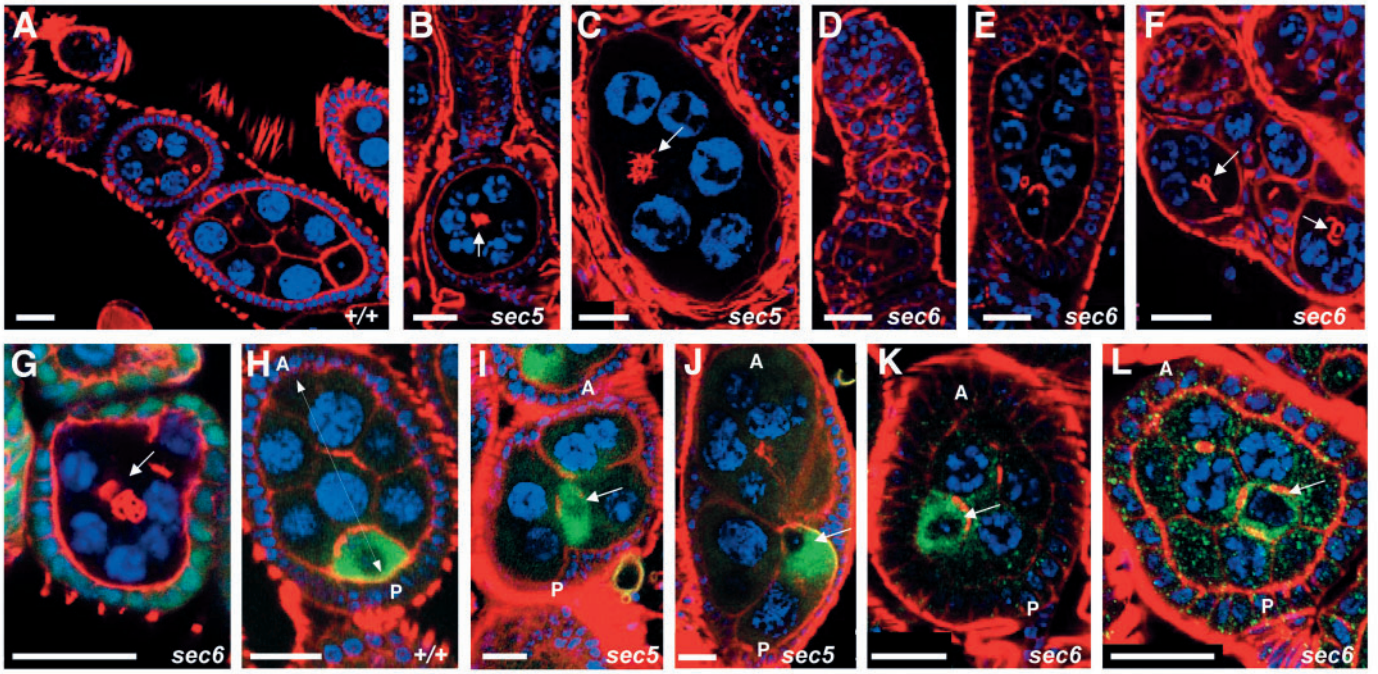

Fig. 5. The *sec5*^{E10} and *sec6*^{Ex15} mutants have similar phenotypes in the ovary. (A-G) Egg chambers labeled with phalloidin (red), Hoechst 33342 (blue) and GFP (green in G). Unlike in the wild type (A), egg chambers from *sec5*^{E10} germ-line clones (B,C) lack membranes (marked with phalloidin) between nuclei and have ring canals clumped together (arrows). Egg chambers from *sec6*^{Ex15} germ-line clones (D-G) exit the germarium and progress through stage 3 (D,E), initially resembling the control. However, after stage 3 (F,G), ring canals clump together (arrows) and phalloidin-marked membranes between nuclei are absent. *FRT42D sec6*^{Ex15} homozygous germ lines were generated by mitotic recombination in combination with either *FRT42B ovo*^{D} (D-F) or *FRT42D Ubi-GFP* and imaging egg chambers that lacked GFP in the germ line (G). (H-L) Egg chambers labeled with Texas Red-phalloidin (red), Hoechst 33342 (blue) and anti-Gurken antibody (green). Gurken accumulates only in the oocyte, which resides at the posterior end of the egg chamber throughout oogenesis, contacting the posterior follicle cells in the wild type (H). In egg chambers from *sec5*^{E10} (I,J) and *sec6*^{Ex15} (K,L) germ-line clones, the oocyte is often mispositioned anteriorly (arrows). Anterior (A) and posterior (P) ends of the chamber are marked. All scale bars are 20 μm.

(P<0.0001) of control, respectively. The amount of induced mCD8 at the cell surface, normalized to the induced amount of GFP, was reduced in the mutant to 37% of control (P=0.1903). The overall reduction of mCD8 at the cell surface in the mutants therefore probably arises from two factors: a decrease in the amount of mCD8-GFP produced in response to RU486 and a defect in trafficking the protein to the plasma membrane.

Although the results of this assay suggest that there is a trafficking defect in *sec6* larvae, the amount of mCD8-GFP expression was so low in the mutants that the specificity and significance of the defect was uncertain. The poor expression of the reporter might be due either to a problem with consumption of the RU486 or to a defect in protein synthesis. We therefore fed *sec6* larvae RU486 at 48 hours AEL, instead of at 72 hours AEL, in the hope that the mutants would be healthier. However, in animals that were fed RU486 at 48 hours AEL for 12 hours, we did not observe a significant trafficking defect (n=7 for both mutant and wild type; data not shown), possibly because there was sufficient maternally contributed Sec6 at this earlier stage. Overall, the phenotypes of *sec5* and *sec6* are fundamentally similar with regard to the trafficking of this reporter protein.

The *sec6* germ-line clones phenocopy *sec5* in the ovary

We generated clones of the *sec6*^{Ex15} allele in the female germ line in order to compare the ovarian phenotype with that of *sec5*^{E10} (Murthy and Schwarz, 2004). As with *sec5*, these mothers did not lay eggs, because the *sec6* allele was lethal to the developing germ-line cells. Moreover, the cellular phenotype was examined with phalloidin to visualize F-actin on membranes and found to be very similar, although less severe, than the *sec5*^{E10} phenotype (Fig. 5B-G). Egg chambers normally consist of 16 germ-line cells linked by cytoplasmic bridges termed ring canals and enclosed within an epithelium of follicle cells. In *sec6*^{Ex15} germ lines, however, egg chambers formed and exited the germarium but, after stage 3, cell membranes were frequently absent between the cells and ring canals that should reside in those membranes were instead clumped together in the middle of a large multinucleate cell (Fig. 5F,G).

When individual cells could be distinguished within the egg chamber, defects were observed in the positioning of the oocyte. In the wild type, the oocyte invariably assumes the posteriormost position among the group of 16 germ cells (Fig. 5H). Similar to *sec5*^{E10}, when the germ line is mutant for *sec6*^{Ex15}, the oocyte is often mispositioned (Fig. 5I-L).

Sec5 protein is mislocalized in *sec6*^{Ex15} germ lines and HA-Sec8 is mislocalized in both *sec6*^{Ex15} and *sec5*^{E13} germ lines

Because Sec5 is dynamically localized to particular regions of the developing oocyte plasma membrane (Murthy and

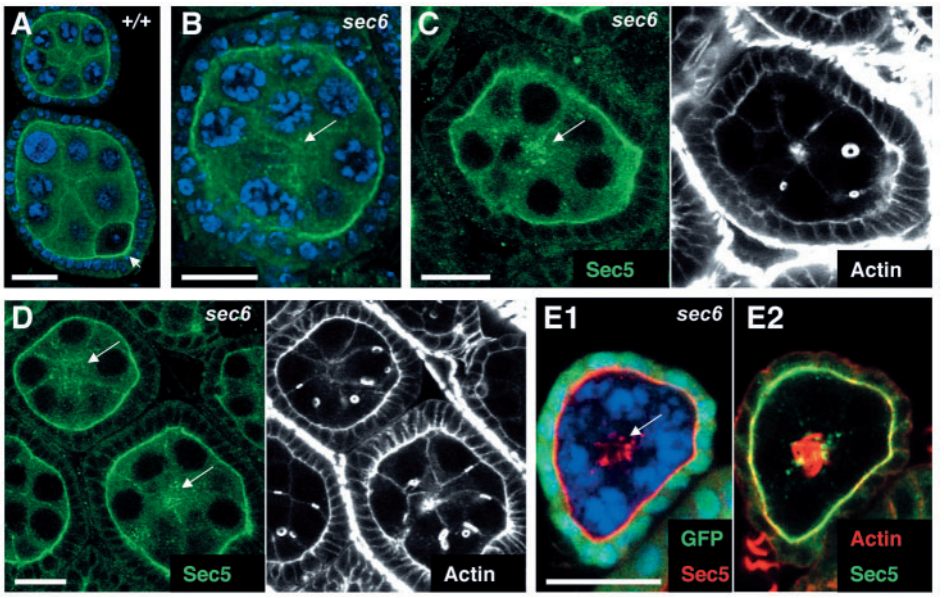

Fig. 6. Sec5 protein is mislocalized in *sec6*^{Ex15} germ-line clones. (A) Control egg chamber, stages 3 and 4, labeled with anti-Sec5 antibody (green) and Hoechst 33342 (blue). Sec5 concentrates on membranes and is enriched at the boundary between the oocyte and posterior follicle cells (arrow). (B) In *sec6*^{Ex15} germ lines, labeled as in A, Sec5 protein is found in puncta (arrow), many of which are clustered towards the center of the egg chamber. (C,D) Sec5 localization (green) is compared with the submembranous actin cytoskeleton (gray) in *sec6*^{Ex15} germ lines. (E1) *GFP*$^{-}$ *sec6*^{Ex15} germ lines (generated as in Fig. 5G) stained for Sec5 (red) and Hoechst 33342 (blue). GFP is shown in green. (E2) *GFP*$^{-}$ *sec6*^{Ex15} germ lines stained for Sec5 (green) and actin (red). (B-E) Sec5 accumulates in intracellular puncta (arrows) and any germ-line membranes separating nuclei have a patchy, discontinuous distribution of Sec5. The Sec5 puncta often accumulate near the clump of ring canals. All scale bars are 20 μm.

Schwarz, 2004), the ovary provided an additional opportunity to test the hypothesis that Sec5 localization depends on Sec6 function. At early stages of wild-type oogenesis, prior to the time when development arrests in *sec6*^{Ex15} germ lines, Sec5 is found principally on the plasma membrane of the 16 cells (Fig. 6A). Moreover, Sec5 is enriched on the oocyte membrane at its posterior edge. In the *sec6*^{Ex15} germ lines Sec5 was mislocalized, with an excess of punctate staining within the cytoplasm of the cells (Fig. 6B-E). In *sec5*^{E10} mutant germ lines, membrane markers such as anti-syntaxin antibody and a fluorescently tagged lectin also label cytoplasmic puncta within the egg chamber, and these puncta are likely to represent fragments of membrane amidst the disrupted cells (Murthy and Schwarz, 2004). The punctate Sec5 immunoreactivity in *sec6* germ lines might similarly represent membrane fragments. Sec5 staining is not, however, completely lost from the boundary of the *sec6* germ-line cells, although much of this might represent Sec5 in the follicle cells, which are heterozygous for the *sec6* mutation.

To compare further the distribution of exocyst components, we generated an HA-tagged Sec8 upstream activation sequence (UAS) construct and expressed this transgene specifically in the *Drosophila* germ line using the *nanos-GAL4* promoter. The transgene did not prevent normal oocyte development and the distribution of the tagged Sec8 was then compared with that of Sec5 (Murthy and Schwarz, 2004). Although little expression of the transgene was detectable at early stages of oogenesis, the two components of the exocyst had parallel distributions at later stages. During stages 7 and 8, Sec5 is localized along the oocyte and nurse-cell membranes, with a slight concentration at anterior corners of the oocyte (i.e. where the lateral membranes of the oocyte meet the anterior surface) (Fig. 7A); at this stage, HA-Sec8 is localized similarly (Fig. 7B). By stage 10, Sec5 is highly enriched at the anterior corners of the oocyte membrane, and we observed a similar distribution for HA-Sec8 (Fig. 7C-E). However, whereas a double line of staining is visible with anti-Sec5 antibody, representing both follicle-cell and oocyte membranes, HA-Sec8 is present only on the oocyte membranes, because the *nanos* promoter does not transcribe the transgene in the follicle cells. When expressed exclusively in the follicle cells of stage-9 egg chambers (using a *GR1-GAL4* driver), HA-Sec8 was again concentrated on the plasma membrane, particularly at the apical end (data not shown). Thus, the distribution of this exocyst component paralleled that of Sec5 in both the oocyte and follicle cells. As with Sec5, the anterior localization of HA-Sec8 in the oocyte was not dependent on microtubules, because it persisted in colcemid-treated females (data not shown). In one regard, however, the distribution of HA-Sec8 differed from that of endogenous Sec5: we frequently observed that individual nurse cells (but not the oocyte) would contain an exceptionally high concentration of HA-Sec8 (Fig. 7B). This might be due to abnormal overexpression of the transgene by *nanos-Gal4*. Indeed, we have observed the same irregular accumulation of several other proteins in nurse cells when expressed from transgenes under the control of *nanos-Gal4* (N.D. and T.S., unpublished).

To examine the dependence of Sec8 localization on Sec5, we expressed the transgene in a *sec5* mutant background. We wished to examine stages 7-10, when the HA-Sec8 localization is clearest, and so looked at germ lines homozygous for the hypomorphic allele *sec5*^{E13} (Fig. 7F-H). In doing so, we uncovered a genetic interaction between Sec8 and Sec5. Females with *sec5*^{E13} germ lines can lay eggs, although membrane trafficking defects in these oocytes result in aberrant dorsal appendages (Murthy and Schwarz, 2004). The overexpression of HA-Sec8, which had no deleterious effect on wild-type oogenesis, enhanced the phenotype of *sec5*^{E13} alone by arresting egg-chamber development between stages 7 and 9, such that no eggs were deposited by these females. Within these germ lines, the oocyte nucleus had migrated appropriately to the anterior end of the cell (at stage 7). However, the oocytes failed to enlarge properly, remaining comparable in size to the nurse cells. Moreover, some disorder of the nurse-cell membranes was apparent, with some cells fused and ring canals clustered together.

HA-Sec8 no longer concentrated at the membrane in *sec5*^{E13} oocytes and was instead uniformly localized throughout the cytoplasm (Fig. 7G,H). This was seen even in those oocytes whose structure was otherwise most normal, with an anterior nucleus and normal membrane-associated actin. By contrast, HA-Sec8 in wild-type oocytes was mostly membrane-associated throughout oocyte development (Fig. 7B).

To examine the dependence of Sec8 localization on Sec6, we expressed the *HA-Sec8* transgene, under the control of *nanos-GAL4*, in a *sec6*^{Ex15} mutant background, by generating *sec6* homozygous germ-line clones. In these clones, HA-Sec8 accumulated in puncta within the egg chamber cytosol (Fig. 7I,J), akin to the Sec5 mislocalization phenotype in *sec6*^{Ex15} egg chambers (Fig. 6). We did not observe an enhancement of the *sec6*^{Ex15} phenotype when HA-Sec8 was overexpressed, but this might be because the *sec6*^{Ex15} phenotype is already quite severe.

Discussion

Whereas the description of exocyst function in *Drosophila* was previously limited to mutations in and antibodies to Sec5, the *sec6* mutations and epitope-tagged form of Sec8 presented here allow a comparison of the distribution and phenotype of additional components of the complex. As summarized below, the data generally favor a model in which these components function as a unit and depend on one another for their localization.

The localization of complex members is consistent with their function as an integral unit. The distribution of Sec5 has been examined most closely in the ovary. In this tissue, it was present on all membranes early in the development of the egg chamber. At late stages, however, Sec5 acquired a characteristic distribution not reported for any other cellular component – a progressive enrichment at the anterior end of the lateral oocyte membranes. HA-Sec8 has now been found to be similarly concentrated in this area, suggesting that several (and perhaps all) exocyst components will be similarly localized.

We also find that mutations in one complex member appear to disrupt the localization of others. Thus, in *sec5*^{E13} homozygous oocytes, HA-Sec8 was no longer membrane bound or concentrated at the anterior sites. Instead, it appeared to fill the cytoplasm diffusely. Similarly, Sec5 was mislocalized within the nervous

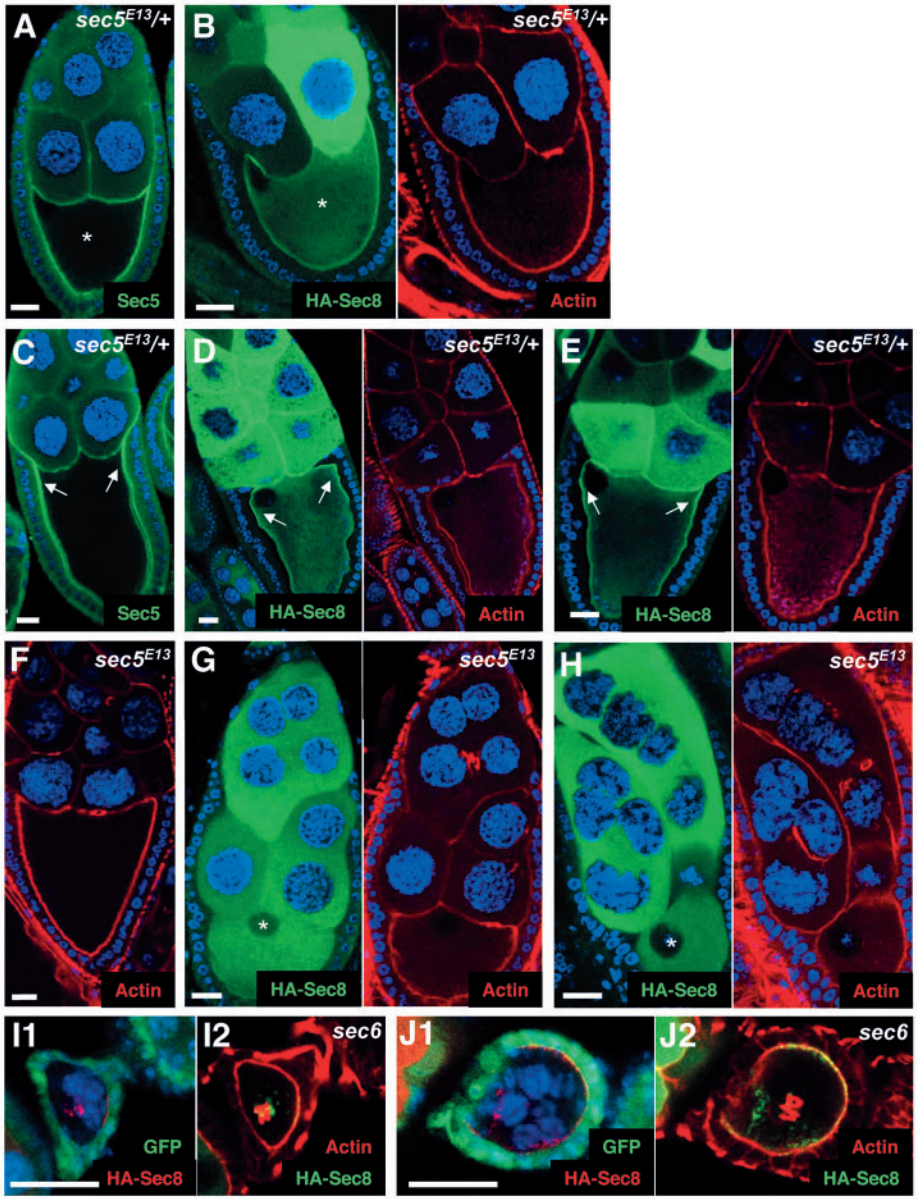

Fig. 7. HA-Sec8 localization in late-stage egg chambers. HA-Sec8 was expressed exclusively in the germ line under the control of *nanos-Gal4*. (A,B) Egg chambers from *sec5*^{E13}/+ heterozygous controls at stage 7 are labeled with anti-Sec5 antibody (A) or anti-HA antibody and Texas-Red/phalloidin (B). Sec5 and HA-Sec8 both concentrate along the oocyte (*) membrane. Probably owing to overexpression, HA-Sec8 often accumulates in the cytoplasm of some nurse cells. (C-E) Egg chambers from *sec5*^{E13}/+ heterozygous controls at stage 10 are labeled with Hoechst 33342 and anti-Sec5 antibody (C) or anti-HA antibody and Texas Red-phalloidin (D,E). Sec5 and HA-Sec8 concentrate at anterior corners (arrows) of the oocyte membrane. (F-H) Egg chambers from *sec5*^{E13} homozygous germ lines are labeled with Hoechst 33342 and Texas Red-phalloidin (F-H) and with anti-HA antibody (G,H). HA-Sec8 no longer concentrates at the oocyte (*) membrane but rather fills the oocyte cytosol when Sec5 function is compromised by the mutation. In addition, the *sec5*^{E13} phenotype (F) is enhanced by the presence of the *HA-sec8* transgene (G,H), stunting the oocyte, disrupting nurse cell membranes and causing ring canals to clump together. (I,J) *GFP*$^{-}$ egg chambers from *FRT42D sec6*^{Ex15} homozygous germ lines, generated by mitotic recombination with *FRT42D Ubi-GFP*. GFP is shown in green (I1,J1). HA-Sec8 (red in I1,J1 and green in I2,J2) accumulates in puncta within the mutant egg chambers and in proximity to actin-rich ring canals (red in I2,J2). All scale bars are 20 μm.

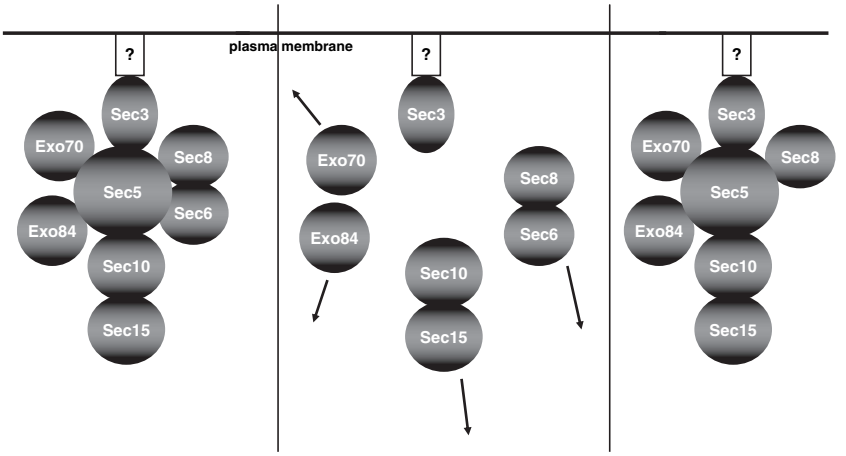

Fig. 8. Organization of the exocyst complex. Interactions are depicted for members of the exocyst complex with each other and with an unknown receptor on the plasma membrane (left), based on a slight modification of the model derived from studies in yeast (Guo et al., 1999) and in accordance with the data from Figs 6, 7. In *sec5* mutants, Sec8 is no longer associated with the membrane and other subunits might also become cytosolic (center). In *sec6* mutants, however, both Sec5 and Sec8 can remain membrane associated (right).

system of *sec6* mutant larvae and Sec5 and HA-Sec8 were both mislocalized within germ lines homozygous for *sec6*. The mislocalization of Sec5 and HA-Sec8 in *sec6* germ lines, however, was not identical to the mislocalization of HA-sec8 in *sec5* germ lines. Whereas the latter involved a diffuse filling of the cytoplasm with immunoreactivity, the mislocalized Sec5 and HA-Sec8 remained punctate within the *sec6* egg chambers. Because these puncta resembled syntaxin and lectin-staining in *sec5* germ lines, it seems likely that they represent fragments of membrane or transport vesicles that have not fused with the plasma membrane. The difference in these two phenotypes might arise from any of several causes, including the perdurance of some Sec6 in the $sec6^{Ex15}$ mutant germ lines. It is tempting to speculate, however, that the difference reflects the organization of proteins within the complex (Fig. 8). Sec3p has been shown in yeast to bind to the plasma membrane at the bud tip even when other complex members are absent (Finger et al., 1998). This has been interpreted as indicating that Sec3p binds directly to a membrane protein and that the localization of other complex members is dependent on Sec3p. Sec5p is thought to bind directly to Sec3p (Guo et al., 1999) and so it is plausible that, in the present study, Sec5 remained membrane bound via its direct interaction with Sec3 even in the absence of Sec6. Sec8, however, is not thought to interact directly with Sec3. Because Sec8 appears to remain membrane-associated in *sec6* but not *sec5* mutants, we hypothesize that a partial complex consisting of Sec3, Sec5 and Sec8 remains on the membrane even in the absence of Sec6. The disposition of the remaining complex members in the *sec5* and *sec6* mutants must remain speculative until suitable reagents have been obtained for their localization.

The interdependence of the complex members is also evident in the genetic interaction of Sec8 and Sec5: although germ-line expression of HA-tagged Sec8 had no phenotype of its own, it enhanced the germ-line phenotype of $sec5^{E13}$, making this partial loss-of-function allele more similar to the null allele. This observation requires that the epitope-tagged transgene be used with caution, because its expression might interfere with exocyst function owing either to an influence of the epitope tag or to unphysiological expression levels. Indeed, phenotypes have been associated with the overexpression of Sec10, another complex member (Lipschutz et al., 2000; Lipschutz et al., 2003).

The phenotypes of *sec6* and *sec5* mutants can be compared in several regards. Like *sec5*, *sec6* caused lethality at approximately 96 hours AEL and these larvae were stunted in their growth and did not progress beyond the first instar. In an assay of membrane-protein transport to the cell surface of identified neurons, we found trafficking defects for *sec6* that were akin to those of *sec5*. In the germ line, we found that membranes between cells disintegrate in *sec6* clones, a phenotype we previously observed for the null allele of *sec5* (Murthy and Schwarz, 2004). For *sec5*, we hypothesized that, as the cells of the germ line grow and expand, membrane addition cannot keep pace, and that membranes between nurse cells and the oocyte consequently fall apart. A similar explanation is likely for *sec6*. We also observed the mispositioning of the oocyte within the *sec6* germ line. Previously, we had shown that this phenotype occurred when either the germ line or the posterior follicles were mutant for *sec5*. Because the positioning of the oocyte is dependent on E-cadherin and cell-cell signaling between the oocyte and follicle cells (Godt and Tepass, 1998; Gonzalez-Reyes and St Johnston, 1998), it is likely that this phenotype arises from a defect in the expression of E-cadherin or other signaling molecules on the oocyte surface. In fact, E-cadherin and Nectin 2a have been recently shown to be binding partners for the exocyst complex in MDCK cells (Yeaman et al., 2004).

Although the similarities of their phenotypes suggest that Sec5 and Sec6 share functions, we observed some differences in the mutant phenotypes. $sec6^{Ex15}$ larvae are smaller than $sec5^{E10}$ larvae but germ-line clones of $sec5^{E10}$ have a more severe phenotype in the ovary, arresting earlier and with fewer remaining membranes. The most intriguing difference arose in the mCD8-GFP expression assay: whereas $sec5^{E10}$ larvae were capable of synthesizing the protein but not of expressing it at the cell surface, $sec6^{Ex15}$ larvae expressed only low levels of the protein, which also appeared to be blocked in their transport to the surface. Finally, whereas HA-Sec8 protein was mislocalized in both *sec5* and *sec6* germ-line clones, the patterns of mislocalized protein were distinct. The differences in the mutant phenotypes might arise from minor factors such as the degree of perdurance of protein in the homozygous germ-line clones or the amount or stability of maternal protein deposited in the egg. However, they might also represent legitimate functional distinctions. The most pronounced difference, the different levels of expression of the mCD8-GFP reporter protein, might reflect the fact that Sec6 is required at an earlier step in the synthesis of membrane proteins, in

addition to its requirement (along with Sec5) for insertion at the plasma membrane. Such a role would be consistent with findings that Sec6 and Sec8 have been observed in the TGN, that Sec8 and Sec10 associate with proteins at the TGN and ER, and that overexpression of Sec10 alters membrane-protein synthesis (Lipschutz et al., 2000; Lipschutz et al., 2003; Sans et al., 2003; Yeaman et al., 2001). The general similarities between and severity of the *sec6* and *sec5* phenotypes also do not exclude the possibility that other components will have more restricted roles, particularly given that several GTPases have emerged as binding partners of particular members of the complex and might be either effectors or regulators of those components (Adamo et al., 1999; Brymora et al., 2001; Inoue et al., 2003; Moskalenko et al., 2002; Prigent et al., 2003; Robinson et al., 1999; Sugihara et al., 2002; Walch-Solimena et al., 1997; Zhang et al., 2001).

In contrast to the cell lethality of the *sec5* and *sec6* phenotypes, a *Sec10* RNA-interference construct in *Drosophila* was reported to have very little effect in most tissues, possibly affecting only the secretions of the ring gland cells (Andrews et al., 2002). However, because no antibody is available for *Drosophila* Sec10 and because maternally contributed protein would be unaffected by this construct, the RNA interference might have been ineffective at reducing endogenous Sec10 levels. In light of the broad phenotypes of dominant negative and overexpressed Sec10 in other cell types (Lipschutz et al., 2000; Lipschutz et al., 2003; Prigent et al., 2003), this is a likely explanation of the discrepancy.

In summary, the similarity of localization of Sec5 and HA-Sec8, the interdependency of the complex members for proper localization in this study, the genetic interaction between *HA-Sec8* and *sec5*, and the general similarity of the *sec5* and *sec6* phenotypes suggest that Sec5, Sec6 and Sec8 associate as a complex in *Drosophila*, acting in concert, and that each is crucial for the function of the complex at the membrane. It will be important to examine the localization and phenotypes of the other complex members to determine whether all the complex members do indeed function primarily as part of the intact exocyst. Furthermore, the mutations in *sec5* and *sec6* should provide a useful genetic background for structure function studies with which to test the significance of their individual binding partners and regulators.

This work was supported by NIH grant NS41062 (T.L.S.) and the Howard Hughes Medical Institute (T.S.). N.D. is supported by a fellowship from the Human Frontier Science Program. We thank Y. Nasrullah for technical support and also M. Salanga and the MRRC Imaging Core.

References

Adamo, J. E., Rossi, G. and Brennwald, P. (1999). The Rho GTPase Rho3 has a direct role in exocytosis that is distinct from its role in actin polarity. *Mol. Biol. Cell* **10**, 4121-4133.

Andres, A. J., Fletcher, J. C., Karim, F. D. and Thummel, C. S. (1993). Molecular analysis of the initiation of insect metamorphosis: a comparative study of *Drosophila* ecdysteroid-regulated transcription. *Dev. Biol.* **160**, 388-404.

Andrews, H. K., Zhang, Y. Q., Trotta, N. and Broadie, K. (2002). *Drosophila* Sec10 is required for hormone secretion but not general exocytosis or neurotransmission. *Traffic* **3**, 906-921.

Brymora, A., Valova, V. A., Larsen, M. R., Roufogalis, B. D. and Robinson, P. J. (2001). The brain exocyst complex interacts with RalA in a GTP-dependent manner: identification of a novel mammalian *Sec3* gene and a second *Sec15* gene. *J. Biol. Chem.* **276**, 29792-29797.

Finger, F. P. and Novick, P. (1997). Sec3p is involved in secretion and morphogenesis in *Saccharomyces cerevisiae*. *Mol. Biol. Cell* **8**, 647-662.

Finger, F. P. and Novick, P. (1998). Spatial regulation of exocytosis: lessons from yeast. *J. Cell Biol.* **142**, 609-612.

Finger, F. P., Hughes, T. E. and Novick, P. (1998). Sec3p is a spatial landmark for polarized secretion in budding yeast. *Cell* **92**, 559-571.

Friedrich, G. A., Hildebrand, J. D. and Soriano, P. (1997). The secretory protein Sec8 is required for paraxial mesoderm formation in the mouse. *Dev. Biol*. **192**, 364-374.

Godt, D. and Tepass, U. (1998). *Drosophila* oocyte localization is mediated by differential cadherin-based adhesion. *Nature* **395**, 387-391.

Gonzalez-Reyes, A. and St Johnston, D. (1998). The *Drosophila* AP axis is polarised by the cadherin-mediated positioning of the oocyte. *Development* **125**, 3635-3644.

Guo, W., Grant, A. and Novick, P. (1999). Exo84p is an exocyst protein essential for secretion. *J. Biol. Chem*. **274**, 23558-23564.

Haarer, B. K., Corbett, A., Kweon, Y., Petzold, A. S., Silver, P. and Brown, S. S. (1996). *SEC3* mutations are synthetically lethal with profilin mutations and cause defects in diploid-specific bud-site selection. *Genetics* **144**, 495-510.

Hsu, S. C., Ting, A. E., Hazuka, C. D., Davanger, S., Kenny, J. W., Kee, Y. and Scheller, R. H. (1996). The mammalian brain rSec6/8 complex. *Neuron* **17**, 1209-1219.

Inoue, M., Chang, L., Hwang, J., Chiang, S. H. and Saltiel, A. R. (2003). The exocyst complex is required for targeting of Glut4 to the plasma membrane by insulin. *Nature* **422**, 629-633.

Lipschutz, J. H., Guo, W., O'Brien, L. E., Nguyen, Y. H., Novick, P. and Mostov, K. E. (2000). Exocyst is involved in cystogenesis and tubulogenesis and acts by modulating synthesis and delivery of basolateral plasma membrane and secretory proteins. *Mol. Biol. Cell* **11**, 4259-4275.

Lipschutz, J. H., Lingappa, V. R. and Mostov, K. E. (2003). The exocyst affects protein synthesis by acting on the translocation machinery of the endoplasmic reticulum. *J. Biol. Chem*. **278**, 20954-20960.

Mondesert, G., Clarke, D. J. and Reed, S. I. (1997). Identification of genes controlling growth polarity in the budding yeast *Saccharomyces cerevisiae*: a possible role of *N*-glycosylation and involvement of the exocyst complex. *Genetics* **147**, 421-434.

Moskalenko, S., Henry, D. O., Rosse, C., Mirey, G., Camonis, J. H. and White, M. A. (2002). The exocyst is a Ral effector complex. *Nat. Cell Biol.* **4**, 66-72.

Murthy, M. and Schwarz, T. L. (2004). The exocyst component Sec5 is required for membrane traffic and polarity in the *Drosophila* ovary. *Development* **131**, 377-388.

Murthy, M., Garza, D., Scheller, R. H. and Schwarz, T. L. (2003). Mutations in the exocyst component Sec5 disrupt neuronal membrane traffic, but neurotransmitter release persists. *Neuron* **37**, 433-447.

Novick, P., Field, C. and Schekman, R. (1980). Identification of 23 complementation groups required for post-translational events in the yeast secretory pathway. *Cell* **21**, 205-215.

Prigent, M., Dubois, T., Raposo, G., Derrien, V., Tenza, D., Rosse, C., Camonis, J. and Chavrier, P. (2003). ARF6 controls post-endocytic recycling through its downstream exocyst complex effector. *J. Cell Biol.* **163**, 1111-1121.

Robinson, N. G., Guo, L., Imai, J., Toh, E. A., Matsui, Y. and Tamanoi, F. (1999). Rho3 of *Saccharomyces cerevisiae*, which regulates the actin cytoskeleton and exocytosis, is a GTPase which interacts with Myo2 and Exo70. *Mol. Cell. Biol.* **19**, 3580-3587.

Sans, N., Prybylowski, K., Petralia, R. S., Chang, K., Wang, Y. X., Racca, C., Vicini, S. and Wenthold, R. J. (2003). NMDA receptor trafficking through an interaction between PDZ proteins and the exocyst complex. *Nat. Cell Biol.* **5**, 520-530.

Sugihara, K., Asano, S., Tanaka, K., Iwamatsu, A., Okawa, K. and Ohta, Y. (2002). The exocyst complex binds the small GTPase RalA to mediate filopodia formation. *Nat. Cell Biol.* **4**, 73-78.

TerBush, D. R. and Novick, P. (1995). Sec6, Sec8, and Sec15 are components of a multisubunit complex which localizes to small bud tips in *Saccharomyces cerevisiae*. *J. Cell Biol.* **130**, 299-312.

TerBush, D. R., Maurice, T., Roth, D. and Novick, P. (1996). The exocyst is a multiprotein complex required for exocytosis in *Saccharomyces cerevisiae*. *EMBO J.* **15**, 6483-6494.

Vega, I. E. and Hsu, S. C. (2001). The exocyst complex associates with microtubules to mediate vesicle targeting and neurite outgrowth. *J. Neurosci*. **21**, 3839-3848.

Walch-Solimena, C., Collins, R. N. and Novick, P. J. (1997). Sec2p mediates nucleotide exchange on Sec4p and is involved in polarized delivery of post-Golgi vesicles. *J. Cell Biol.* **137**, 1495-1509.

Yeaman, C., Grindstaff, K. K., Wright, J. R. and Nelson, W. J. (2001). Sec6/8 complexes on trans-Golgi network and plasma membrane regulate late stages of exocytosis in mammalian cells. *J. Cell Biol.* **155**, 593-604.

Yeaman, C., Grindstaff, K. K. and Nelson, W. J. (2004). Mechanism of recruiting Sec6/8 (exocyst) complex to the apical junctional complex during polarization of epithelial cells. *J. Cell Sci.* **117**, 559-570.

Zhang, X., Bi, E., Novick, P., Du, L., Kozminski, K. G., Lipschutz, J. H. and Guo, W. (2001). Cdc42 interacts with the exocyst and regulates polarized secretion. *J. Biol. Chem*. **276**, 46745-46750.